ICRA2026 Late Breaking Results Poster presented at
2026 IEEE International Conference on Robotics and Automation (ICRA 2026)
June 1-5, 2026. Vienna, Austria

Three-dimensional Needle Tip Estimation from Multi-View X-ray Images for Interventional Pain Procedures

Seunghui Han, *Student Member, IEEE*, and Ayoung Hong, *Member, IEEE*

***Abstract*— This study addresses the challenge of estimating the three-dimensional (3D) position of a needle tip from two-dimensional (2D) X-ray images. We propose a classical image processing–based framework for needle tip localization and 3D reconstruction. The method first detects a circular marker attached to the robotic end-effector that controls the needle insertion and identifies the needle head position within the marker. Preprocessing steps, including bilateral filtering, thresholding, and iterative morphological operations, are applied to improve image quality and ensure the continuity of the needle shaft. A flood-fill algorithm is then used to segment the needle body, after which the needle trajectory is extracted using the A* algorithm. Finally, the 3D position of the needle tip is reconstructed by Triangulation from multiple X-ray images acquired at different viewing angles.**

I. Introduction

Estimating the position of the needle tip in real X-ray images presents several challenges. When a 3D structure is projected onto a 2D image, it becomes difficult to preserve the needle's directional information. In addition, X-ray images typically exhibit lower contrast and higher noise levels compared to standard RGB images.

Previous studies have explored bottom-up strategies for reconstructing interventional device shapes from biplane X-ray images, leveraging centerline extraction and epipolar-geometry–based triangulation, with further improvements incorporating graph-based optimization and feature correspondence refinement [1], [2]. Moreover, due to the slender, shaft-shaped geometry of the needle, there are limited discriminative features available for learning-based models. Since the needle occupies only a very small number of pixels within the entire image, it is also prone to being overlooked during training. Furthermore, when the patient's anatomy is captured alongside the needle, other linear structures (e.g., blood vessels or bones) may be misidentified as the needle due to similar edge characteristics.

To address these challenges, this study proposes a classical image processing–based approach rather than a model-based tracking method. The needle tip is detected in X-ray images, and then its three-dimensional position is estimated using triangulation.

This work was supported by the Technology Innovation Program (20023168, Development of clinician collaborative robot platform technology for 3 types of pain interventional procedures based on crossdrug handler and instrument modules) funded By the Ministry of Trade, Industry & Energy (MOTIE, Korea)

Seunghui Han and Ayoung Hong are with the Department of Mechanical Engineering, Chonnam National University, Gwangju 61186, Republic of Korea ahong@jnu.ac.kr

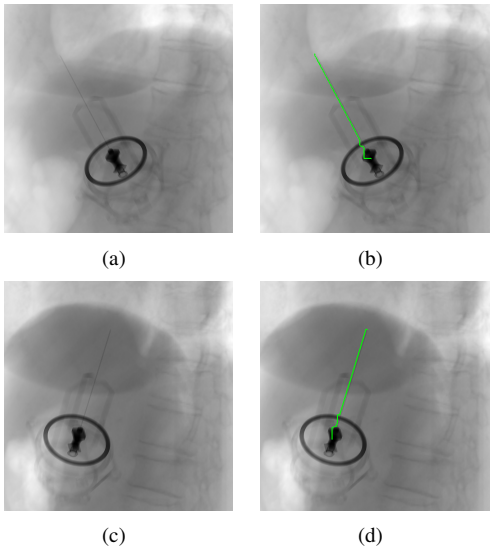

Fig. 1. Comparison before and after Image Processing in generated DRR image: (a) projected image in rotation 60°, (b) after image processing projected image in rotation 60°, (c) rotated 120°, and (d) after image processing projected image in rotation 120°

II. Needle Tip Estimation

A. Image Processing algorithm

First, to enable real-time tracking and improve computational efficiency, the input image is resized to 640 × 640. The image is then uploaded to the GPU, and a bilateral filter is applied as a preprocessing step to reduce noise while preserving edges.

To localize the marker, its circular characteristic is exploited by detecting an ellipse in the image. Within the detected marker region, the pixel with the highest intensity value is selected as the needle head position. Afterward, thresholding is performed, followed by iterative erosion and dilation to ensure continuity of the thin needle shaft without fragmentation.

Next, using the previously identified needle head as the seed point, a flood-fill algorithm is applied to obtain the segmentation of the needle body. Finally, the needle head is defined as the start point and the needle tip as the end point, and the A* algorithm is used to compute the path along the needle shaft.

B. Triangulation

The DRR imaging system is modeled as a perspective projection where the X-ray source corresponds to the camera

center. 3D points are reconstructed via linear triangulation using two DRR views with known projection matrices.

$$\tilde{\mathbf{x}} = \mathbf{P}\tilde{\mathbf{X}} \tag{1}$$

where $\tilde{\mathbf{x}} = [u, v, 1]^T$ and $\tilde{\mathbf{X}} = [X, Y, Z, 1]^T$ are homogeneous coordinates of the 2D and 3D points, respectively. The projection matrix $\mathbf{P} \in \mathbb{R}^{3\times4}$ is $\mathbf{P} = \mathbf{K}[\mathbf{R} \mid \mathbf{t}]$.

The translation vector is defined from the X-ray source position $\mathbf{C}$ as:

$$\mathbf{t} = -\mathbf{R}\mathbf{C} \tag{2}$$

Given two views, the 3D point $\mathbf{X}$ is estimated by solving:

$$\mathbf{A}\mathbf{X} = 0 \tag{3}$$

where

$$\mathbf{A} = \begin{bmatrix} u_1\mathbf{P}_1^{(3)} - \mathbf{P}_1^{(1)} \\ v_1\mathbf{P}_1^{(3)} - \mathbf{P}_1^{(2)} \\ u_2\mathbf{P}_2^{(3)} - \mathbf{P}_2^{(1)} \\ v_2\mathbf{P}_2^{(3)} - \mathbf{P}_2^{(2)} \end{bmatrix} \tag{4}$$

The solution is obtained via SVD, followed by homogeneous normalization.

III. Results

A. Experimental Setups

The experimental setup used in this study is as follows. The GPU employed is an NVIDIA GeForce RTX 3060, and the version of OpenCV used is 4.9.0. The DRR images have a resolution of 1536×1536 pixels, and the real X-ray images have a resolution of 1280×1280 pixels.

B. Results on DRR image

To generate DRR images, DeepDRR [3] was utilized. The patient's 3D CT data and the needle mesh file were imported into the framework, and DRR images were generated by configuring the projector parameters, including its position and imaging geometry.

Figure 1 shows the results for the generated DRR images. Figure 1(a) presents a DRR image generated with the C-arm rotated by 60 degrees about the y-axis, while Figure 1(c) presents a DRR image generated with the C-arm rotated by 120 degrees about the y-axis. To evaluate the performance of the 2D imaging process algorithm, the pixel coordinates of the needle tip manually annotated by an expert were used as the ground truth. The error between the ground-truth coordinates and those obtained through image processing was, on average, 4 pixels.

The error of result was computed as the Euclidean distance between the 3D coordinates obtained via Triangulation and the corresponding ground-truth coordinates. The angular separation between the DRR images used for triangulation ranged from 20° to 60°. The mean error was 0.89 mm, with a standard deviation of 0.45 mm.

C. Result from Real X-ray image

The data used in this study consist of real X-ray images acquired in December 2025 at Asan Medical Center in Seoul, under the guidance and supervision of clinical experts. Figure 2 is the image of the result from a real X-ray image. The real X-ray images used in this study were acquired during in vivo animal experiments on a live pig and captured in a clinical setting using a C-arm fluoroscopy system.

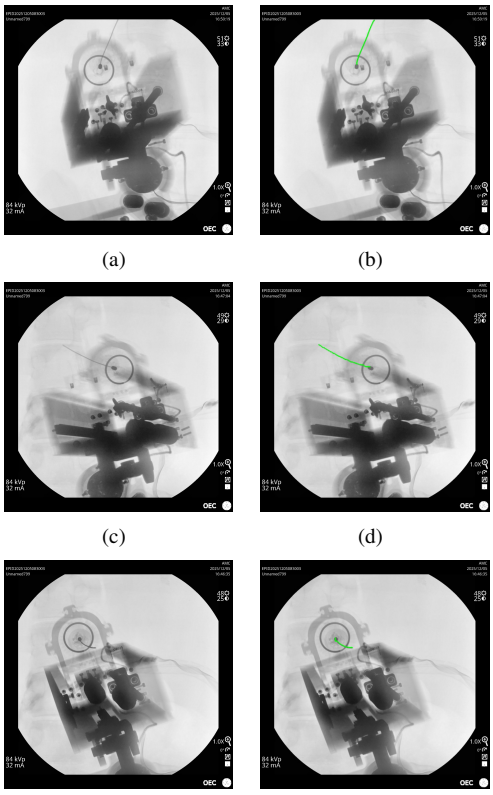

Fig. 2. Comparison before and after Image Processing in Real X-ray image: (a),(c),(e) Before image processing with Real X-ray image, and (b),(d),(f) After image processing with Real X-ray image. The green line is the path of the found needle.

IV. Conclusion

In this study, the needle tip location in X-ray images was estimated using a classical image processing–based approach, and the proposed method was validated on X-ray images obtained from animal experiments. The 3D position of the needle tip was then reconstructed by triangulation from tip locations extracted from images captured at different viewing angles. Future work will focus on improving the robustness of the method under more diverse imaging conditions and extending it to in-vivo environments.

References

[1] J. Burgner, S. D. Herrell, and R. J. Webster III, "Toward fluoroscopic shape reconstruction for control of steerable medical devices," in *Dynamic Systems and Control Conference*, vol. 54761, 2011, pp. 791–794.

[2] M. Wagner, S. Schafer, C. Strother, and C. Mistretta, "4d interventional device reconstruction from biplane fluoroscopy," *Medical physics*, vol. 43, no. 3, pp. 1324–1334, 2016.

[3] B. D. Killeen, L. J. Wang, B. Iñígo, H. Zhang, M. Armand, R. H. Taylor, G. Osgood, and M. Unberath, "Fluorosam: A language-promptable foundation model for flexible x-ray image segmentation," in *Proceedings of MICCAI 2025*, September 2025.